TASK II

Project II.6

COMPUTATIONAL CHEMISTRY OF MODEL COMPOUNDS AND DIRECT LIQUEFACTION CATALYSTS

K.R. Subbaswamy
Department of Physics & Astronomy
University of Kentucky

The two primary tasks undertaken during '92-93 were (i) the initiation of the microscopic study of iron-based direct liquefaction catalysts; and (ii) the completion of the study of radical hydrogen transfer (RHT) as a possible mechanism to explain selective bond cleavage in model compounds .

(i) Modeling of Iron-Based Catalysts

The development of effective, environmentally safe and economical catalysts is the key to making direct coal liquefaction a commercially viable goal. To this end, there has been a great deal of interest in sulfided iron catalysts for coal liquefaction.

Recent experimental results have lead to a greater understanding of the action of these iron-based catalysts. Pradhan, et al.[1] have shown that the presence of sulfur increases the liquefaction conversion and oil yields when starting with sulfated oxides and oxyhydroxides of iron. It is also known[2] that molybdenum is a more active catalyst for liquefaction than iron, that molybdenum produces a more highly hydrogenated product, and that the addition of molybdenum to the iron sulfided catalysts greatly increases the activity of the iron catalyst.[3]

Farcasiu, et al.[4] have observed that the iron-sulfur systems formed in the reaction of many of the fine particle iron oxide catalysts lead to the selective hydrocracking of the bond between a condensed polyaromatic ring and an aliphatic carbon. To explain these results, Walter, et al.[5] have proposed that in the presence of iron-carbonyl based catalyst precursors the iron dissociates hydrogen into atoms which can then insert into the naphthalene system, leading to either hydrogenation or bond cleavage. Also, from kinetic studies of the iron carbonyl catalysts Suzuki[6] suggests that the role of the iron catalyst is to activate molecular hydrogen and transfer hydrogen to coal fragment radicals in a nonhydrogen donor solvent.

Through a charge distribution analysis study, Freund and Whang[7] have observed that the surface of a magnetite catalyst becomes positively charged above 230°C. Between 275-410°C the surface is catalytically active toward dealkylation of 6-methyl-9-(1-methylethyl) dibenzothiophene-4-ol, suggesting that the active

magnetite surface acts as an electron acceptor. By contrast, the hematite surface remains negatively charged up to 450°C.

Microdiffraction patterns of several of the iron-sulfided catalysts suggest that the catalyst crystal is Fe_7S_8 in the $[001]_{hcp}$ orientation.[8] Montano, et al.[9] have proposed that the catalytic activity of pyrrhotites is the result of iron vacancies, and that hydrogen sulfide is necessary to maintain a surface with iron deficient sites.

We have investigated, through quantum chemical modeling, the possible action of an FeS catalyst toward a hydrogen molecule and other simple molecules such as toluene, as well as the influence of vacancies on such processes. Not many quantum chemical computational methods can handle large numbers of transition metal atoms. The ASED-MO method developed by A.B. Anderson,[10,11] has been used by us in the study of the possible cleavage mechanisms of model compounds of interest to investigators in the field of direct coal liquefaction.[12-15] Anderson has used the method to study ethylene hydrogenation mechanisms on Pt surfaces and ethylene and acetylene absorption on MoS_2 clusters.[16,17] This method has also been used by Je and Companion[18] to explain the Fischer-Tropsch catalytic properties of various Co surfaces. In the method one models a surface by a small number of atoms (i.e., such as the surface of a cluster of atoms). Thus, this method is ideal for the study of the small ultrafine particle catalysts and can possibly address whether the departure from bulk properties when the catalyst size approaches 10 nm is the cause of catalytic activity.[19]

The ASED-MO energy of adsorption of the species on the surface was calculated by computing the difference between the ASED-MO energy of the molecule adsorbed on the surface and the energy of the molecule and surface at infinite separation:

$$\text{Adsorption energy} = E_{\text{surface-adsorbate}} - (E_{\text{surface}} + E_{\text{adsorbate}}).$$

As defined here, a negative adsorption energy indicates an exothermic adsorption.

The bond dissociation energy (BDE) was found by computing the difference in the ASED-MO energies between the surface-adsorbate complex and the surface-radical complex and methyl-radical energies at infinite separation. As defined for the adsorption of toluene, the BDE expression would read

$$BDE = (E_{CH_3\bullet} + E_{\text{surface}\bullet C_6H_5\bullet}) - E_{\text{surface-adsorbate}\bullet}$$

As can be seen, the bond dissociation energy will depend on the stability of the surface-radical complex as well as the bond strength as predicted by the overlap population of the adsorbed species. No optimization of either of the two free radical species formed upon bond cleavage was done, so these bond dissociation energies should be considered an upper bound to the 'true' value.

We have investigated the adsorption of simple aromatic ring compounds on three

different faces of an FeS cluster and on a pyrrhotite cluster. FeS has a hexagonal NiAs structure, with each Fe atom in an octahedral environment of S atoms.[20] The packing is a(Fe)-b(S)-a(Fe)-c(S). Pyrrhotite exhibits a similar structure with iron vacancies in alternate layers.[21] Above 308°C pyrrhotite does not exist as a single crystal structure, but exhibits "a rather wide homogeneity range as a single solid solution $Fe_{1-x}S$ with the NiAs structure, extending from the stoichiometric FeS to a composition of approximately $Fe_{0.81}S$."[22] The Neél (antiferromagnetic ordering) temperature of FeS is 327°C. It should be noted that most of the liquefaction experiments are carried out above 350°C.[23] Thus, magnetic effects should not be relevant for the catalytic activity.

The first cluster we investigated is shown in Figure 1 and consists of 19 Fe atoms in the top layer, 12 sulfur atoms in the second layer and 19 iron atoms in the third layer for a total of 50 atoms. This face (0001) is hereafter referred to as the smooth face. This particular cluster was chosen in our initial studies because of its simplicity. The interatomic distances were chosen to correspond to those in an idealized pyrrhotite structure. The nearest neighbor distance between iron atoms in the same layer is 3.43 Å but 2.84 Å between layers. The Fe-S distance is 2.44 Å. This is to be compared with the nearest neighbor distance in bcc pure iron of 2.48 Å. While this cluster does not have the overall stoichiometry of FeS, it is representative of the correct stoichiometry in the immediate vicinity of the adsorption sites studied.

The adsorption of toluene was also investigated on a $(11\bar{2}0)$ surface. This two layer cluster, shown in Figure 2, consists of zig-zag chains of alternating Fe and S atoms and contains 28 S atoms and 20 Fe atoms for a total of 48 atoms. We have also investigated adsorption properties when the surface layer consists of sulfur atoms only. The surface of this FeS $(10\bar{1}0)$ cluster can be described as containing stepped layers of sulfur atoms. The cluster contains 27 Fe atoms and 25 S atoms for a total of 52 atoms. We have modeled the pyrrhotite structure by creating Fe vacancies in the smooth FeS cluster, as described below.

We have investigated the adsorption of toluene and 1-methylnaphthalene on the smooth FeS surface. A typical minimized geometry of the adsorbate with respect to the surface is shown in Figure 3. In this calculation the ring carbon atom of the $C_{aromatic}$-$C_{aliphatic}$ linkage was initially placed directly above the Fe atom in the center of the cluster. In all of the calculations the methyl group is oriented with one hydrogen down towards the surface and the other two up, as is shown in Figure 3.

Our computed results for the adsorption energy, BDE, and charge transfer for the smooth surface are summarized in Table 1. The adsorption energy of toluene to the surface is exothermic by 3.05 eV and that of 1-methylnaphthalene by 5.47 eV. With the parameters used, we observe the transfer of electron charge from the adsorbed molecules to the FeS cluster with a resultant decrease in the C_{ring}-CH_3 overlap population and bond breaking energy as compared to unabsorbed toluene and 1-methylnaphthalene. The transfer of charge for 1-methylnaphthalene was greater than that for toluene. The bond dissociation energy for toluene decreases upon

chemisorption from 4.25 to 2.99 eV and for 1-methylnaphthalene from 4.20 to 2.89 eV. Using unabsorbed toluene and 1-methylnaphthalene as reference points, it is observed that electron density is removed from the p_z (π) orbitals of the ring system and from the σ bond of the C_{ring}-$C_{aliphatic}$ linkage, thereby weakening the affected bond.

The adsorption of toluene was also investigated on a $(11\bar{2}0)$ surface. No stable adsorption site for toluene was found when the ring carbon of the C_{ring}-CH_3 linkage was initially placed above an Fe atom of this surface. However, a very weak adsorption was observed when the center of the aromatic ring was placed above an iron atom of the surface. The adsorption occurs at a distance 3.0 Å above the surface, and the adsorption energy is 0.09 eV. No charge transfer from toluene to or from the surface is observed and the charge density on the atoms in the toluene molecule resemble that of free toluene. No stable adsorption site for toluene was found on the stepped $(10\bar{1}0)$ surface with sulfur exposed when the ring carbon atom of the C_{ring}-CH_3 was placed directly above a surface sulfur atom.

In order to simulate the pyrrhotite iron deficient structure, the Fe atom under the ring carbon of the C_{ring}-CH_3 linkage was removed, thereby creating a vacancy. Toluene is not as strongly adsorbed in this case as in the pristine cluster; the energy of adsorption decreases to 1.95 eV. Also, the bond dissociation energy increases to 3.23 eV. As in the centered case, electron density is removed from the π orbitals of the aromatic system but not from the σ bond linkage.

Transition metal sulfides are used extensively as hydrotreating catalysts. To investigate the effect of FeS in such processes, we have studied the adsorption of H_2 on FeS clusters. When a hydrogen molecule is placed parallel to the stepped surface, one hydrogen atom directly above a sulfur atom and at a distance of 2.4 Å from the surface we find that the hydrogen molecule escapes from the vicinity of the surface as a hydrogen molecule. However, when the hydrogen molecule was pushed down to 1.4 Å above an exposed sulfur atom, as might occur under pressure, the hydrogen molecule dissociates and forms a pseudo-H_2S species on the surface of the stepped surface. The optimized geometry after dissociation has a H-S-H bond angle of 106° and a H-S bond distance of 1.4 Å.

We find that a hydrogen molecule (with the molecular axis parallel to the surface) is weakly physisorbed above an Fe atom on the smooth surface. No tendency for dissociation of the hydrogen molecule into hydrogen atoms is found.

Rodriguez and Baker[24] have recently undertaken a systematic study of the interaction of iron sulfides with hydrogen in the presence of graphite. Through an *in situ* diffraction analysis they observed the formation of pits on the graphite surface already at room temperature, even when the iron sulfide particles were not directly in contact with it. Our preliminary results suggest that reactive species are formed by the chemisorption of H_2 on certain FeS surfaces. Further work is needed to investigate whether the species so formed are released easily from the surface.

We observe that molecules with aromatic ring systems are strongly chemisorbed by Fe atoms of the FeS (0001) catalyst surface only, suggesting that there is a critical number of exposed Fe atoms necessary in order for stable adsorption to occur. Polycondensed aromatic ring compounds are more strongly adsorbed than monocyclic ring compounds. With the parameters used in the calculations, a transfer of charge from the molecule to the catalyst is observed, creating a radical cation-substrate complex and leading to a decrease in bond dissociation energies of bonds between aromatic rings and aliphatic carbons. This appears to be similar to the mechanism proposed by Farcasiu, et al.[25] in the context of the catalytic decomposition of 4-(1-naphthylmethyl)bibenzyl in the presence of carbon black.

(ii) Radical Hydrogen Transfer Mechanism

We had previously investigated radical hydrogen transfer (RHT) as a possible mechanism to explain the selective cleavage of C-C bonds in model compounds. In RHT a hydrogen atom is transferred from a solvent derived radical to the ipso position of an aryl-alkyl linkage of the substrate, followed by elimination of the substituent. Free hydrogen transfer may also compete with the RHT process.

In our earlier modeling RHT was studied by the addition of atomic hydrogen directly to various sites in Model I. During the current year, we extended these studies to include the transfer of hydrogen from a $C_6H_7\bullet$ radical (modeling a solvent derived radical) to the various aromatic sites in Model I. The three stages in our modeling are shown in Figure 5. The AM1 semiempirical method (within RHF with half-electron correction for radicals) was used as before.

Potential energy curves were calculated for the transfer of the hydrogen atom from the $C_6H_7\bullet$ radical in two different ways. In one series of calculations (referred to as series A below) the $C_6H_7\bullet$ radical was allowed to approach Model I until the energy started becoming repulsive. At this point the distance between the radical and Model I was held constant, and the transfer of H between the two components allowed to occur. In the other (referred to as series B) the $C_6H_7\bullet$ radical was allowed to approach Model I with no constraints along the transfer path. From the potential energy curves the barrier height for H atom transfer at positions 1-4 on Model I as labeled in Figure 6 were determined. Also, the bond dissociation energies for the dissociation of the corresponding (Model I - H)$\bullet$ radical was computed. Then, assuming that the hydrogen transfer is the rate determining step, the expected end product distributions were calculated and compared with the experimental results of Farcasiu, et al.[25] The results for the barrier for addition or transfer of hydrogen are compared in Table 2. It is seen that the barrier heights do not predict the preferential cleavage of the polycyclic aromatic-aliphatic linkage to be kinetically favored. The RHT mechanism as modeled in our study does not appear to explain the selective cleavage of Model I.

References

1. Pradhan, V.R .; Hu, J.; Tierney, J.W.; Wender, I. *Prepr., Div. Fuel Chem., Am. Chem. Soc.* **1993**, *38(1)*, 8.

2. Derbyshire, F.; Hager, T. Prepr., *Div. Fuel Chem., Am. Chem. Soc.* **1992**, *37(1)*, 312.

3. Pradhan, V.R.; Herrick, D.E.; Tierney, J.W.; Wender, I. *Energy & Fuels*, **1991**, *5*, 712.

4. Farcasiu, M.; Eldredge, P.A.; Petrosius, S.C. Prepr., *Div. Fuel Chem., Am. Chem. Soc.*, **1993**, *38(1)*, 53.

5. Walter, T.D.; Casey, S.M.; Klein, M.T.; Foley, H.C. *Prepr., Div. Fuel Chem., Am. Chem. Soc.*, **1993**, *38(1)*, 46.

6. Suzuki,T. *Prepr., Div. Fuel Chem., Am. Chem. Soc.*, **1993**, *38(1)*, 137.

7. Freund, F.; Whang, E.-J. Prepr., *Div. Fuel Chem., Am. Chem. Soc.*, **1993**, *38(1)*, 172.

8. Srinivasan,R.;Keogh, R.A.; Davis, B.H. Prepr., *Div. Fuel Chem., Am. Chem. Soc.*, **1993**, *38(1)*, 203.

9. Montano, P.A.; Stenberg, V.I.; Sweeny, P. *J. Phys. Chem.*, **1986**, *90*, 156.

10. Anderson, A.B. *J. Chem. Phys.*, **1974**, *60*, 2477.

11. Anderson, A.B. *J. Chem. Phys.*, **1975**, *62*, 1187.

12. Ades, H.F.; Companion, A.L.; Subbaswamy, K. R. *J. Phys. Chem.*, **1991**, *95*, 2226.

13. Ades, H.F.; Companion, A.L.; Subbaswamy, K. R. *Prepr., Div. Fuel Chem., Am. Chem. Soc.*, **1991**, *36*, 420.

14. Ades, H.F.; Companion, A.L.; Subbaswamy, K. R. *J. Phys. Chem.*, **1991**, *95*, 6502.

15. Ades, H.F.; Companion, A.L.; Subbaswamy, K. R. (to be published).

16. Yu.J.; Anderson, A.B. *J. Mol. Catal.*, **1990**, *62*, 223.

17. Anderson, A.B.; Choe, S.J. *J. Phys. Chem.* **1989**, *93*, 6145.

18. Je, Y.-T.; Companion, A. *Surf. Sci. Letters*, **1992**, *271*, L345.

19. Eklund, P.C.; Stencel, J.M.; Bi, X.-X.; Keogh, R.A.; Derbyshire, F.J. Prepr., *Fuel Chem. Div., Am. Chem. Soc*, **1992**, *37*, 551.

20. Evans, R.C.; *An Introduction to Crystal Chemistry*, Cambridge University Press, **1966**.

21. Fleet, M.E. *Acta Cryst.*, **1971**, *B27*, 1864.

22. Rao, V.U.S. *Prepr., Div. Fuel Chem., Am. Chem. Soc.*, **1993**, *38(1)*, 184.

23. *AIP Handbook of Physics, 3rd edition*, 1972, ed. by D.E. Gray, McGraw-Hill, p.5-173.

24. Rodriguez, N.M.; Baker, R.T.K. Prepr., *Div. Fuel Chem., Am. Chem. Soc.*, **1993**, *38(1)*, 80.

25. Farcasiu M. and Smith, C. *Energy & Fuels*, **1991**, *5*, 83.

Figure Captions

Figure 1. Top and side views of FeS (0001) cluster studied. The smaller spheres are the sulfur atoms and the larger spheres are iron atoms. The sphere sizes are not meant to represent the actual sizes of the atoms.

Figure 2. The zig-zag $(11\bar{2}0)$ FeS cluster studied. The zig-zag chains on the top layer are marked.

Figure 3. Top and side views of toluene adsorbed on the smooth FeS (0001) surface.

Figure 4. Dissociation of the H_2 molecule on the stepped FeS $(10\bar{1}0)$ surface.

Figure 5. The modeling of hydrogen transfer from the $C_6H_7\bullet$ radical to Model I.

Figure 6. The site labels for Model I used in Table 2.

(a) Top View

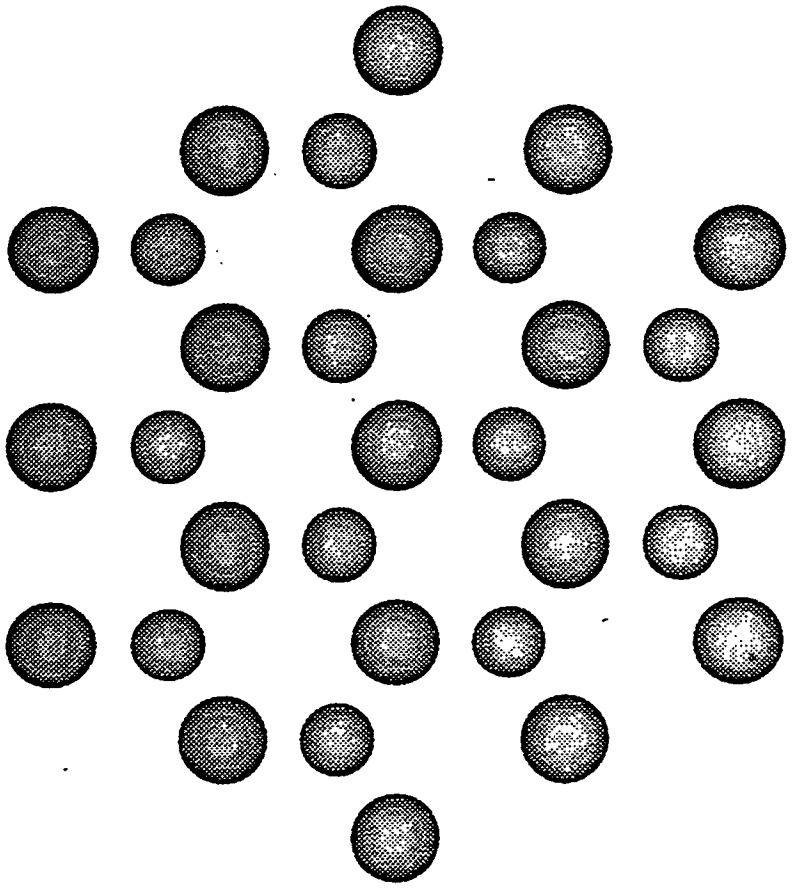

(b) Side View

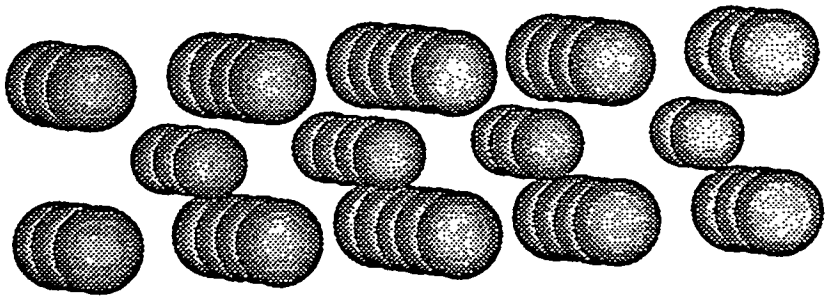

FIGURE 1

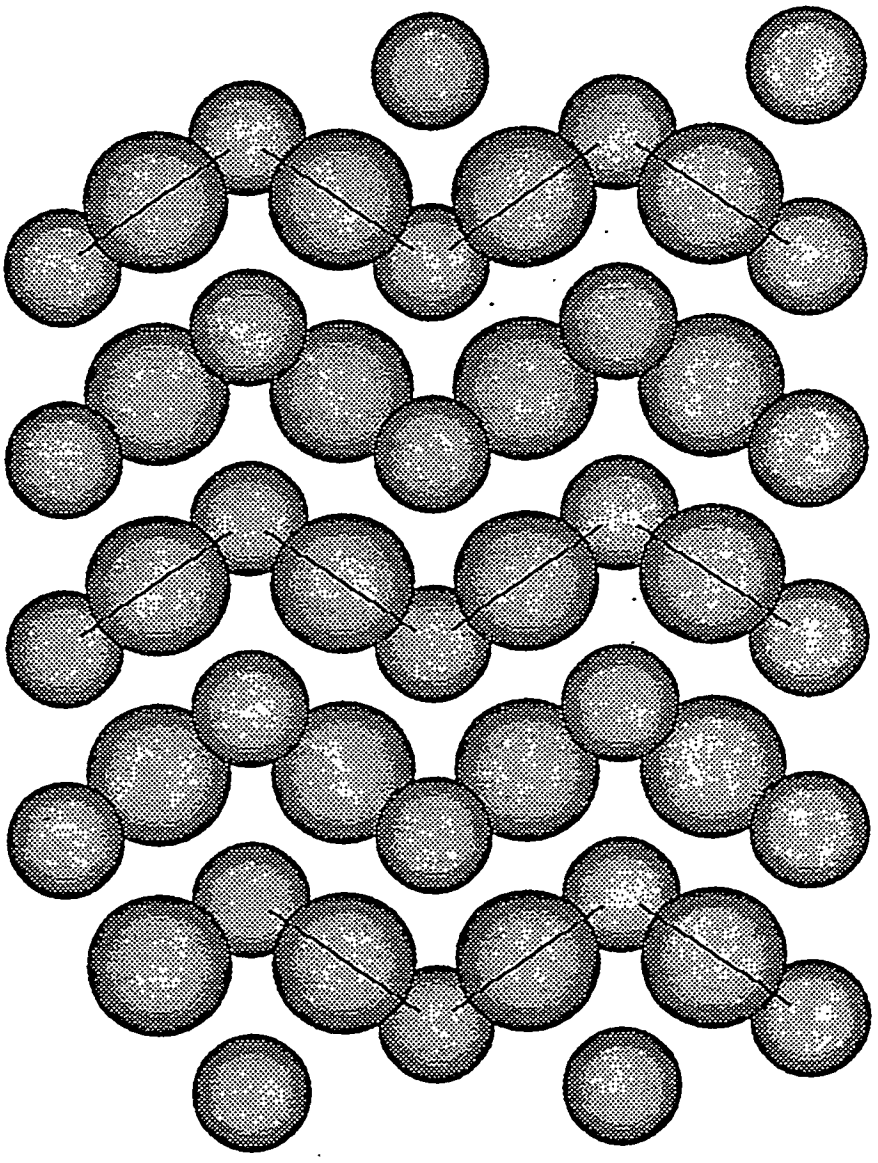

FIGURE 2

(a) Top View

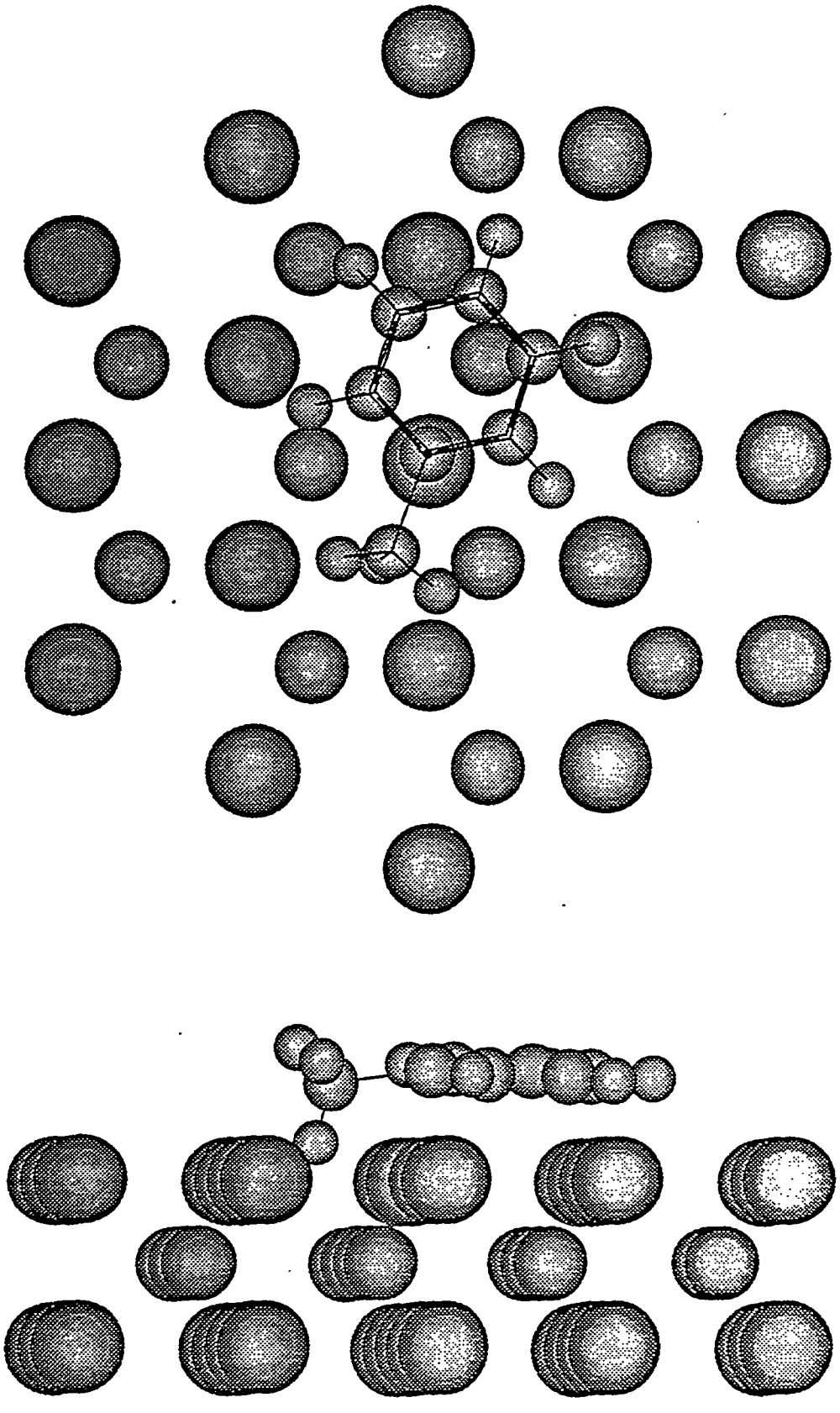

(b) Side View

FIGURE 3

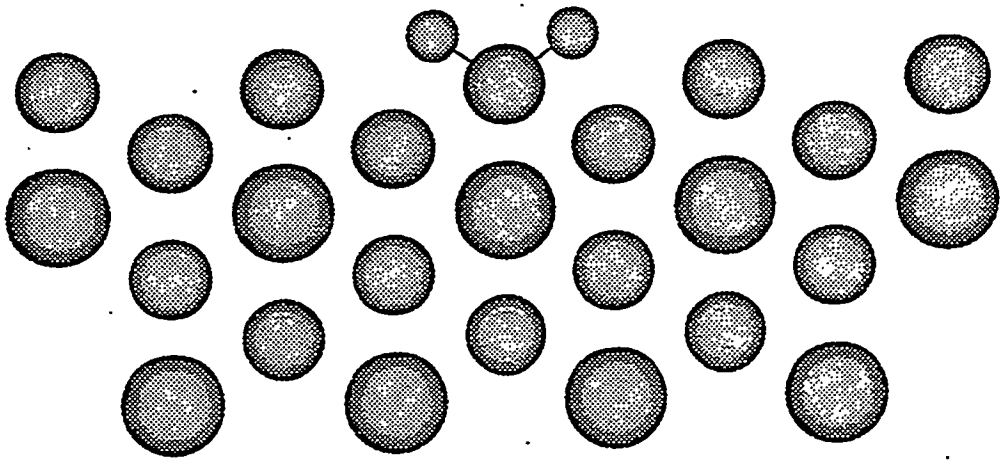

Figure 4

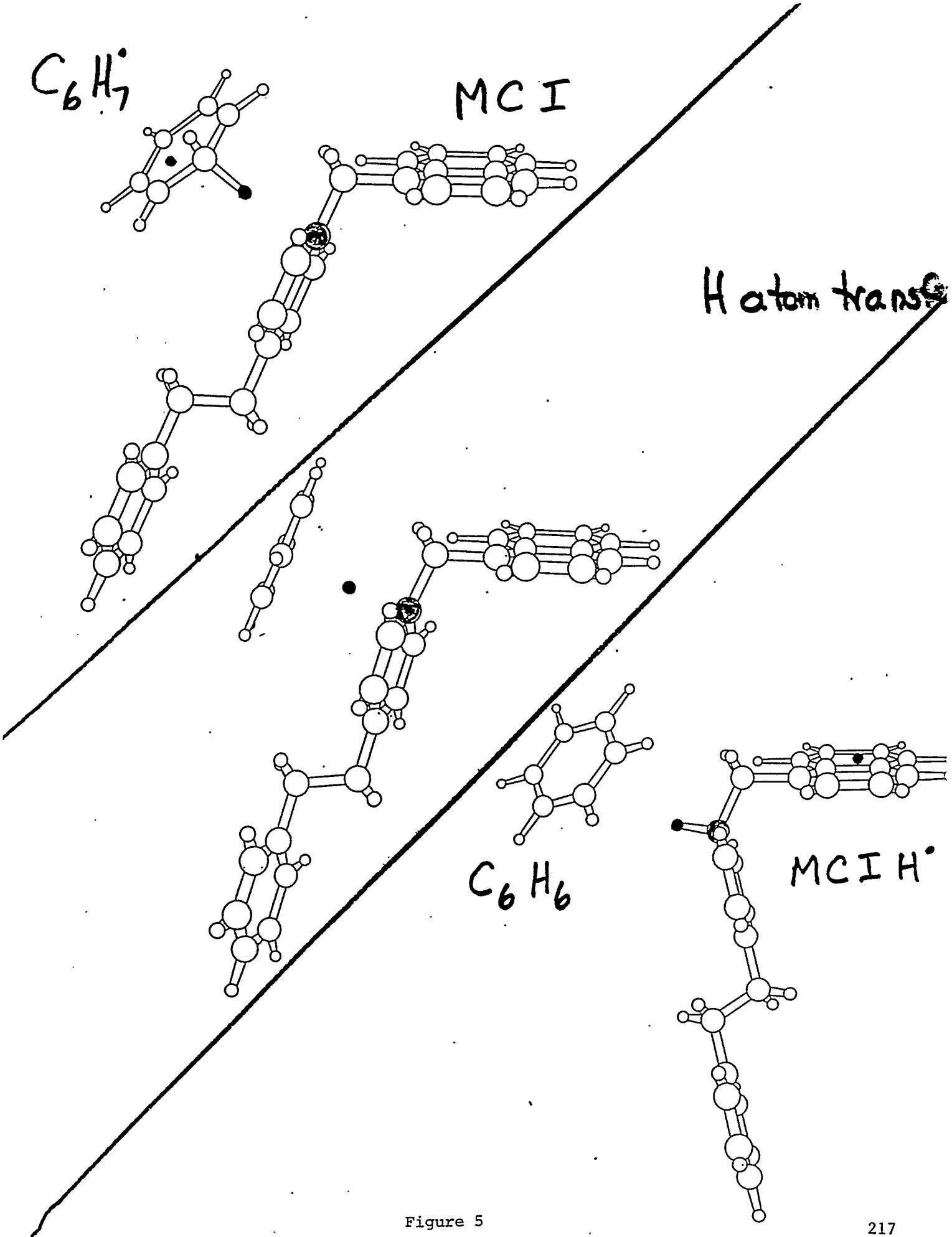

Figure 5

Site	Free		Over Fe		Centered	Over Vacancy
Species	Toluene	1-methyl N	Toluene	1-methyl N	Toluene	Toluene
$-E_{adsb.}$			3.05	5.47	3.89	1.95
BDE	4.25	4.20	2.99	2.89	3.23	3.23
ΔQ to surface			$0.87e^-$	$1.68e^-$	$0.75e^-$	$0.55e^-$
$\Delta\rho_e$ from $C_{aromatic}$			0.1587	0.2036	0.1406	0.0875
$\Delta\rho_e$ from $C_{aliphatic}$			0.0663	0.0520	0.0005	-0.0006

Table 1 Summary of results of adsorption of toluene and 1-methylnaphthalene (1-methyl N) on FeS (0001) surface. Results for free (unadsorbed) species are included for comparison. ΔQ is the charge transfer to the surface; the last two rows give the total electron density removed from the aromatic carbon and the aliphatic carbon of the $C_{aromatic}$-$C_{aliphatic}$ linkage, respectively.

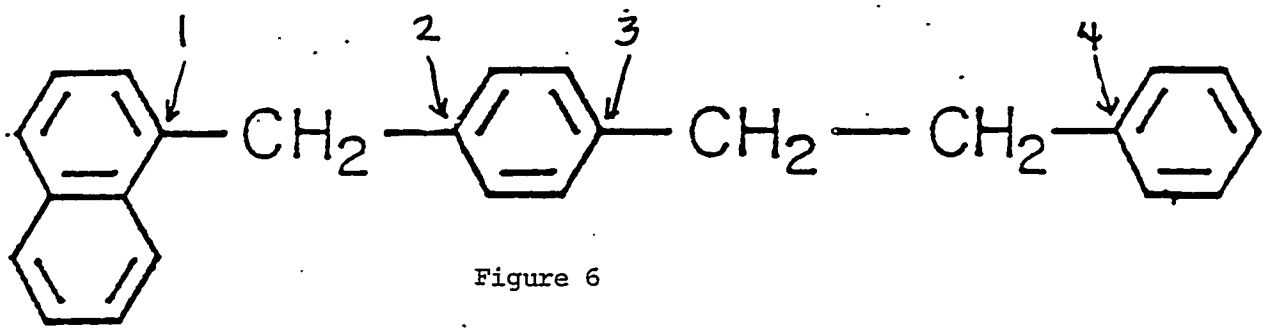

Figure 6

Barrier Heights (eV)

Pos.	H addition	H transfer A	H transfer B
1	0.53	1.88	1.98
2	0.44	1.89	1.76
3	0.44	1.88	1.74
4	0.55	1.88	1.72
d_{M1-H} at highest energy	1.78Å	1.75Å	1.38Å

Table 2. Barrier heights for hydrogen addition (column 2), and hydrogen transfer in method A (column 3) and method B (column4) (see text). The position labels are given in Figure 6.

TASK II

Project II.7

CHEMICAL CHARACTERIZATION AND HYDROGENATION REACTIONS OF SINGLE COAL PARTICLES

Asit Ray
University of Kentucky

No report was submitted.